Alaska DOT&PF Pile Extension Pier Pushover Software Version 1.0 Installation Instructions and Theory Documentation

FINAL REPORT

Prepared for
Alaska University Transportation Center and
Alaska Department of Transportation and Public Facilities

Michael H. Scott
Oregon State University
School of Civil and Construction Engineering
Corvallis, OR 97331
Report # FHWA-AK-RD-11-03
February 2011

Contents

List of Figures

Acknowledgments

This work has been supported by the Alaska University Transportation Center (AUTC), under US Department of Transportation award DTRT06-G-0011, and the Alaska Department of Transportation and Public Facilities as AUTC Project Number 107013. Any opinions expressed in this material are those of the author and do not necessarily reflect the views of the funding agencies.

Abstract

AASHTO is developing seismic bridge design provisions using an explicit displacement-based methodology where a bridge's lateral displacement capacity is compared directly to demands induced by seismic events (earthquakes) through a pushover analysis. This represents a departure from past and current AASHTO guidelines where an approximate force-based methodology was employed to design bridges based on the forces generated during a seismic event. The displacement-based approach can lead to improved bridge designs; however, the calculations required for the pushover analysis are difficult for an engineer to perform without the aid of computer software. To adopt the forthcoming AASHTO displacement-based bridge design specifications using tools currently available, AKDOT&PF bridge engineers would have to rely on a patchwork of disparate software plus hand calculations to conduct a pushover analysis. Development and adoption of a single, automated software tool for pushover analysis will reduce the cost of future bridge designs by reducing the amount of time AKDOT&PF engineers spend analyzing bridges for seismic loads.

Summary of Findings

The development approach taken for this software was relatively unique in terms of structural engineering software. The software is built around free components, namely Tcl/Tk, a string-based scripting language with widgets for developing graphical user interfaces (GUIs), and OpenSees, an open source nonlinear finite element analysis software framework. This combination of Tcl/Tk and OpenSees allowed for rapid protoyping of GUIs that interact with state-of-the-art element and constitutive models for the analysis of cast-in-steel shell (CISS) bents. From a computational point-of-vew, very little "from-scratch" coding was required other than a few p-y models, as modules available in OpenSees were repackaged to meet AKDOT&PF's needs. This development approach will be fruitful for future AKDOT&PF software projects and potentially for commercialization and technology transfer. Based on close dealings with Mr. Elmer Marx during its development, the software was found to be generally easy to use for analyzing a wide range of CISS bents in the AKDOT&PF inventory and more efficient compared to the variety of separate software previously used for such analyses.

Chapter 1

Getting Started

The software, zCISS , is developed using the Tcl/Tk scripting languange for model generation and graphical user interfaces in conjunction with OpenSees as its computational engine for nonlinear finite element analysis.

1.1 Installation Instructions

The user is required to install Tcl/Tk version 8.5 or later, which is available free of charge at

`http://www.activestate.com/activetcl`

In addition, the user must have the Tk-version of OpenSees (`OpenSeesTk.exe`) installed, which can also be downloaded for free at

`http://opensees.berkeley.edu`

The combined use of OpenSees and Tcl/Tk makes zCISS platform-independent, with only aesthetic differences in window appearance.

1.2 Startup Instructions

With `OpenSeesTk.exe` and `zCISS.tcl` installed in the same directory, there are two options to start the software under the Windows operating system.

1. Double-click on the `OpenSeesTk.exe` icon. An MS-DOS window will then appear showing OpenSees copyright information along with an interactive prompt. In addition, there will be a plain grey window titled `openSeesTk`, as shown in Figure 1.1. At the prompt in the MS-DOS window, type `source zCISS.tcl` (also shown in the figure). This will cause the plain grey window to change to the zCISS startup window shown in Figure 1.3.

2. Drag the `zCISS.tcl` icon over the `OpenSeesTk.exe` icon, as shown in Figure 1.2 and release. The zCISS startup window shown in Figure 1.3 should appear immediately along with the MS-DOS window showing OpenSees copyright information.

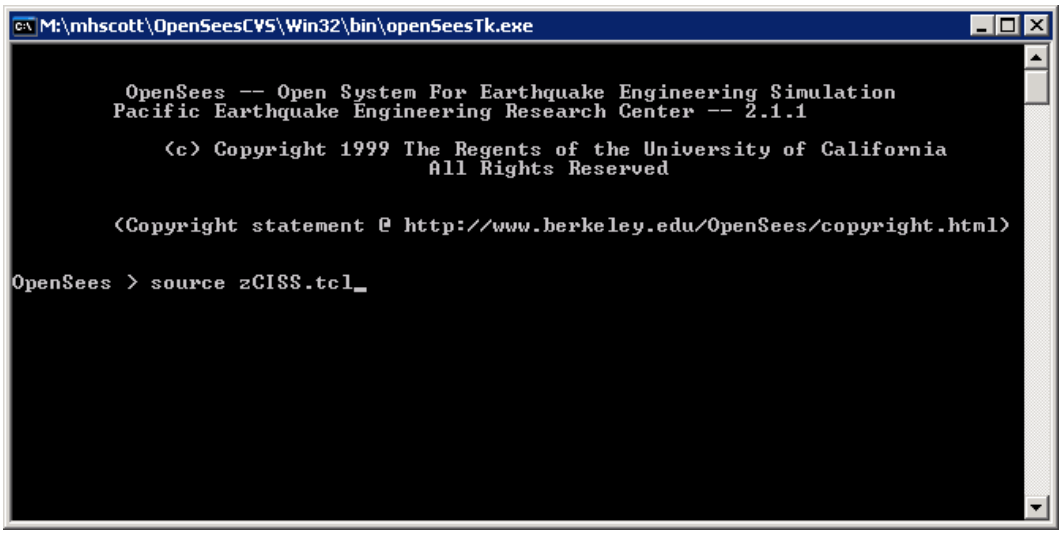

Figure 1.1: MS-DOS window created by double-clicking on the `OpenSeesTk.exe` icon.

1.3 Default Bent Model

Upon startup, the software creates a default bent model with the following basic details shown in Figure 1.3:

- Three 36.0 in diameter columns, 8.0 ft on center, each with 486.1 kip axial load and 2.0 in gap at bent cap;
- Columns 14.0 ft above grade extending 60.0 ft below grade;
- Three 20.0 ft sand layers with water table at 3.0 ft;

Further reinforcing details, soil properties, and analysis options for this default model are omitted from this list for brevity.

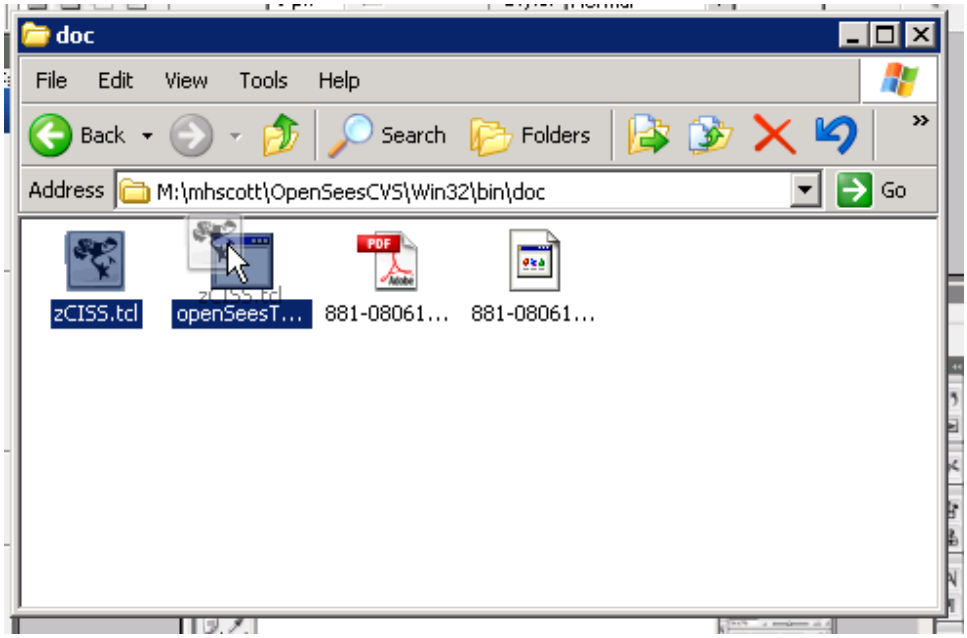

Figure 1.2: Dragging the `zCISS.tcl` icon over the `OpenSeesTk.exe` icon in Windows Explorer.

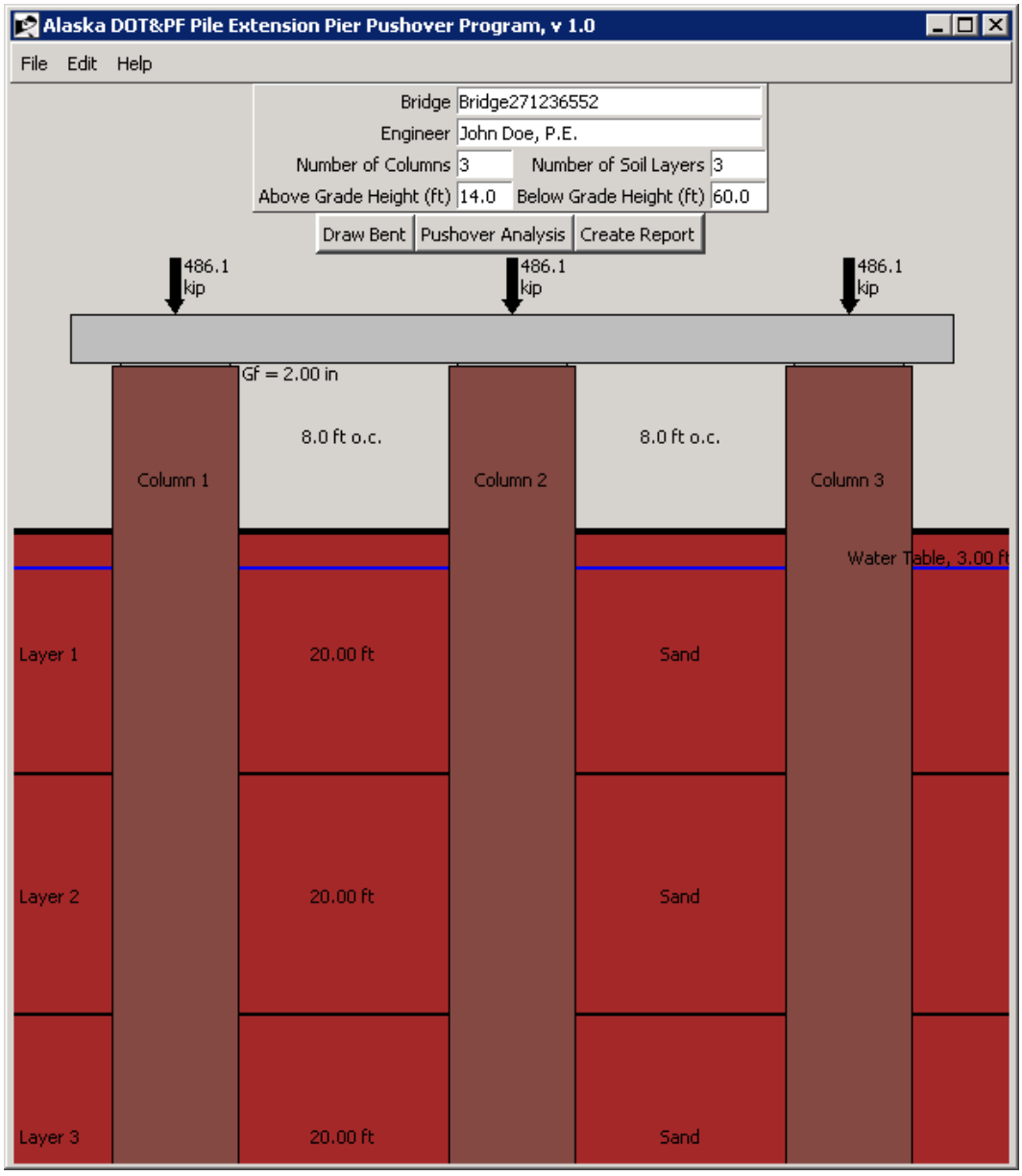

Figure 1.3: Main window created after software is started.

Chapter 2

Finite Element Model

The bridge bent is modelled and analyzed in 2D using nonlinear frame (beam-column) and zero length (spring) elements. The line, or skeleton, idealization of a representative bridge bent is shown in Figure 2.1.

2.1 Column Elements

A single force-based frame element [7] simulates the response of each column member. The cross-section constitutive response is obtained by numerical integration of concrete and steel stress-strain response (fiber section approach). The software creates two fiber sections: one with a steel jacket and one without. The former is used along the entire pile length except for the gap region adjacent to the bent cap. Both sections use the following constitutive models for concrete and steel materials.

2.1.1 Concrete

For unconfined concrete in the gap region, the software uses the Kent-Scott-Park model [4], while it uses the Mander model [5] for confinement owing to the steel jacket below the gap region and spiral hoops in the gap region. Effective lateral confining pressures are calculated for the steel jacket region according to Chai et al [2], while confining pressures of the spiral hoops in the gap region are computed according to Mander [5]. The software's default concrete properties are shown in Figure 2.2(a) with the following definitions:

`f_ce` = expected concrete compressive strength (ksi)

`e_co` = unconfined concrete compressive strain at the maximum compressive stress (in/in)

`e_sp` = ultimate unconfined compression (spalling) strain (in/in)

`f_cc` = confined compressive strength of concrete (ksi)

`e_cc` = compressive strain at maximum compressive stress of confined concrete (in/in)

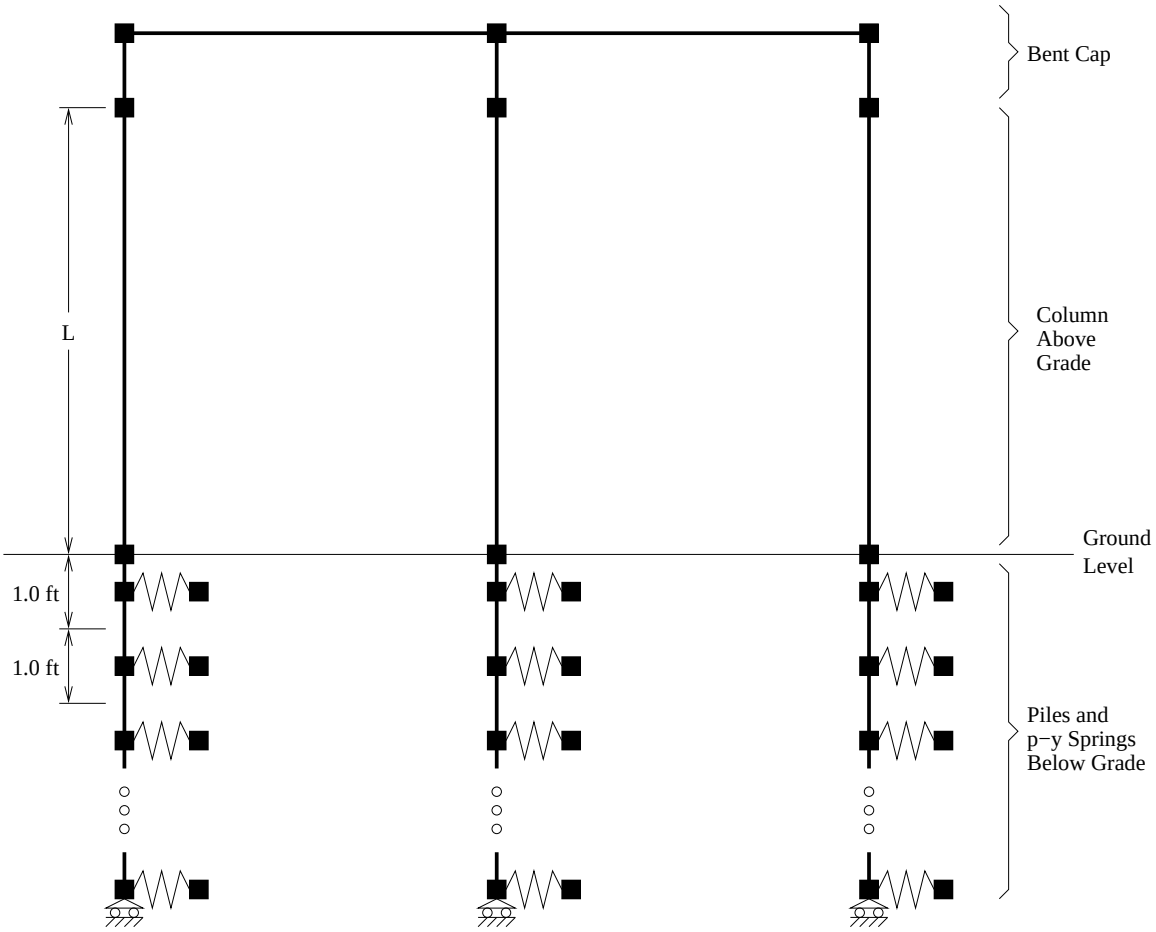

Figure 2.1: Line element idealization of bridge bent system.

Using the default values for unconfined concrete properties shown in Figure 2.2(a), the resulting stress-strain behavior of unconfined, jacket confined, and spiral hoop confined concrete is shown in Figure 2.2(b).

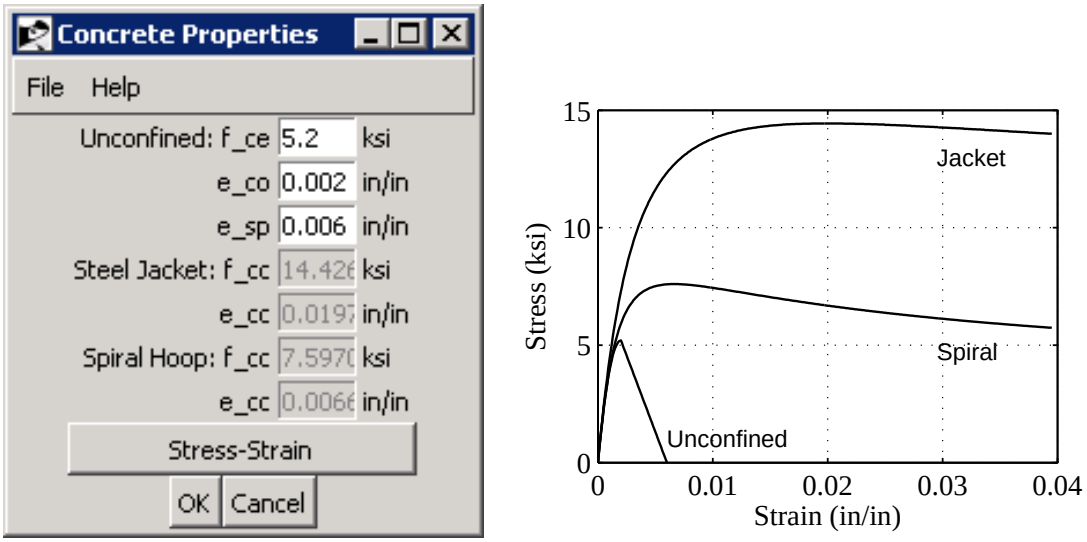

(a) Software defaults

(b) Stress-strain behavior

Figure 2.2: Stress-strain model used for unconfined concrete and concrete confined by steel jacket and spiral hoop reinforcement.

2.1.2 Steel

The steel stress-strain behavior for the longitudinal response of both the reinforcing bars and the jacket is based on the model proposed by Raynor [8]. The software's default properties of longitudinal reinforcing steel are shown in Figure 2.3(a) with the following definitions:

`E` = modulus of elasticity of steel (ksi)

`f_ye` = expected yield strength (ksi)

`f_ue` = expected tensile strength (ksi)

`e_sh` = tensile strain at the onset of strain hardening (in/in)

`e_suR` = reduced ultimate tensile strain (in/in)

`e_su` = ultimate tensile strain (in/in)

`C1` = power curve parameter of Raynor [8] model

Using the default values for longitudinal reinforcing steel shown in Figure 2.3(a), the resulting stress-strain behavior is shown in Figure 2.3(b). Default properties for the jacket steel differ slightly from those shown in Figure 2.3(a) with `f_ye` = 60 ksi, `f_ue` = 78 ksi, `e_suR` = 0.04 in/in, and `e_su` = 0.06 in/in.

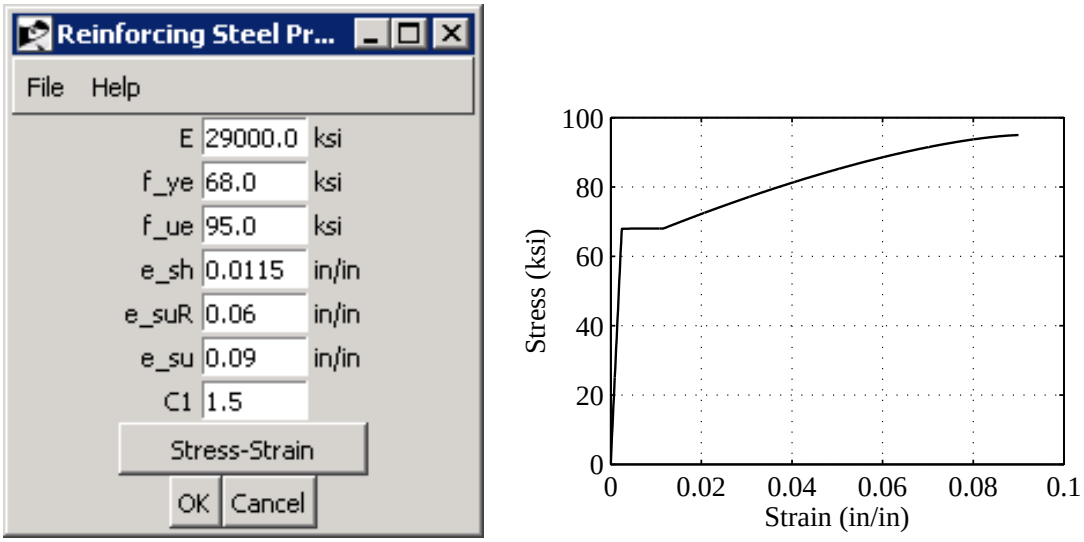

(a) Software defaults

(b) Stress-strain behavior

Figure 2.3: Stress-strain model used for longitudinal response of reinforcing steel.

2.1.3 Plastic Hinge Length

To allow for the possibility of losing lateral load carrying capacity under heavy gravity loads, a regularized integration approach [11] is used along the element length. The plastic hinge length assigned at the top of the column member is based on Eq. (4.11.6) from [1]

$$L_p = G_f + 0.3 f_{ye} d_{bl} \tag{2.1}$$

where G_f is the gap between the isolated flare and the soffit of the bent cap (in), f_{ye} is the expected yield strength of the column longitudinal steel (ksi) (shown in Figure 2.3(a)), and d_{bl} is the nominal diameter of the column longitudinal steel reinforcing bars (in). The plastic hinge length at the column base is set to zero. This selection of integration point locations give four evaluation points along the column height.

2.2 Bent Cap

The bent cap is modeled using linear-elastic frame elements with cross-section properties based on user input of the bent cap width and depth and elastic modulus based on the user

input concrete strength.

$$E_c = 57000\sqrt{f'_{ce}} \qquad \text{(psi)} \tag{2.2}$$

where f'_{ce} is the expected concrete compressive strenth (psi) input via the window of Figure 2.2(a).

2.3 Subgrade Pile Elements

Below grade there is a series of standard displacement-based frame elements whose cross-section response is also obtained by the fiber section approach with two Gauss-Legendre integration points. Each node below grade is connected to a zero length p-y spring element in order to simulate soil resistance to lateral loading of the bent. The vertical spacing of p-y springs is fixed at 1.0 ft, as shown in Figure 2.1. The software includes three types of soil: stiff clay, soft clay, and sand, each with resistance calculated either above or below the water table based on the following parameters:

`gamma` = unit weight of soil (pcf)

`phi` = angle of internal friction (deg)

`c` = soil shear strength (psi)

`eps50` = soil strain corresponding to one-half the maximum principal stress difference (in/in)

`nh` = increase in soil stiffness with respect to depth (pci)

The implementation of each of p-y soil model in OpenSees follows the procedures described in [12], with formulations developed by [10], [6], and [9] for stiff clay, soft clay, and sand, respectively. The behavior of each model, using the software's default values of the parameters listed above, is shown in Figures 2.4, 2.5, and 2.6 for cases 5.5 ft above and 4.5 ft below a hypothetical water table of 10 ft below grade.

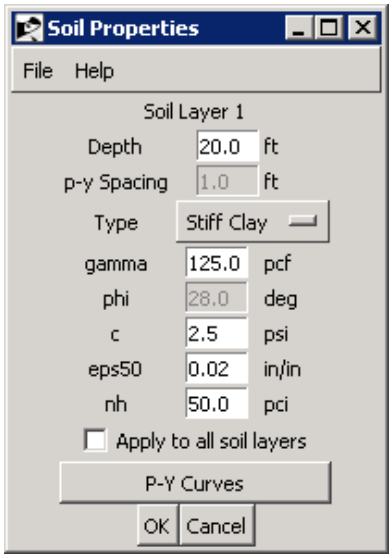

(a) Software defaults

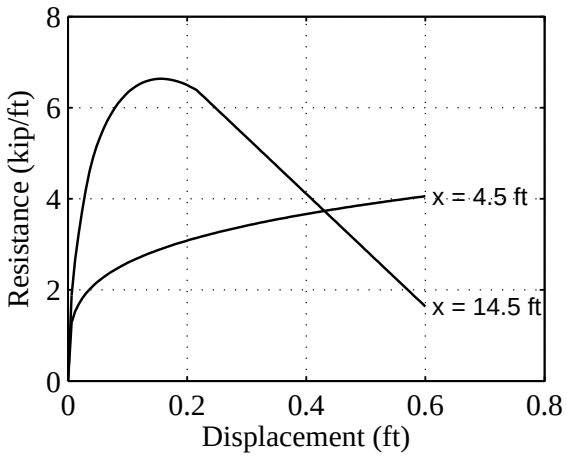

(b) p-y curves

Figure 2.4: p-y model for stiff clay resistance [10] above and below water table at x=10 ft below grade.

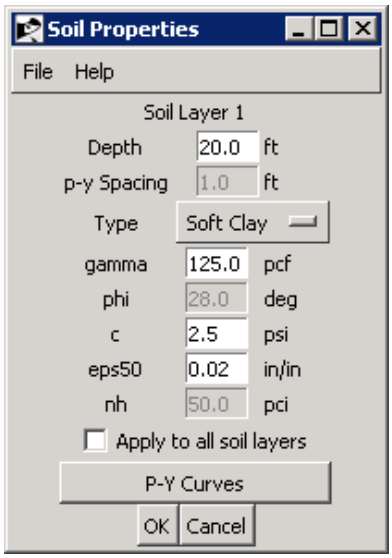

(a) Software defaults

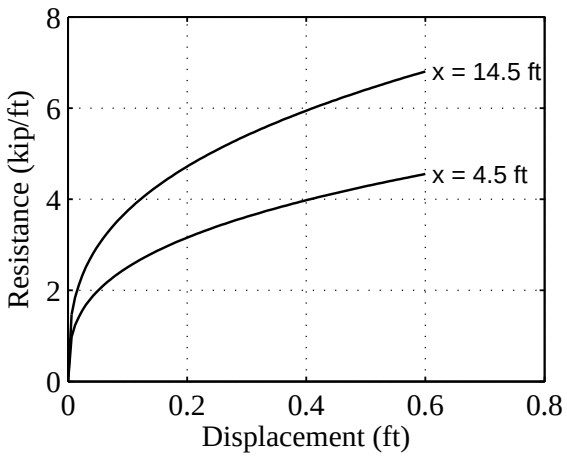

(b) p-y curves

Figure 2.5: p-y model for soft clay resistance [6] above and below water table at x=10 ft below grade.

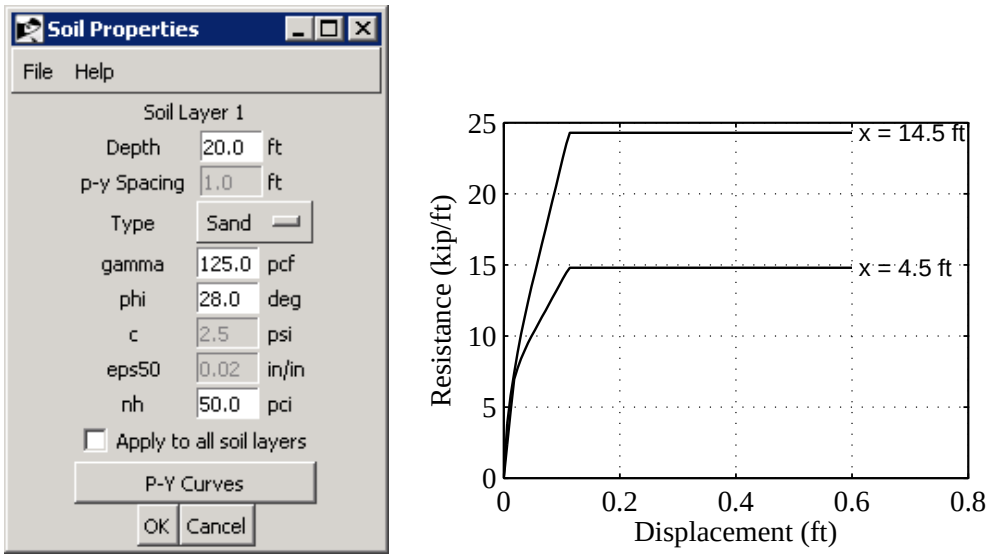

(a) Software defaults

(b) p-y curves

Figure 2.6: p-y model for sand resistance [9] above and below water table at x=10 ft below grade.

2.4 Analysis Options

Several options dictate how the lateral response of the bent model is computed, as well as how the results are displayed on screen, during a pushover analysis. These options, along with their default values, are shown in Figure 2.7 and described below:

- **Max Lateral Displacement** – This is the target lateral displacement at which the analysis terminates under normal conditions.
- **Post Peak Capacity** – Should the lateral response peak, then show a loss in capacity before reaching the maximum lateral displacement, this is the capacity level at which the analysis will terminate.
- **Soil-Structure Interaction** – The radio button turns soil-structure interaction (SSI) on and off. For the "On" selection, the interaction of piles and soil is simulated during the analysis using the previously described nonlinear beam-column elements and p-y springs. In the "Off" selection, the node at ground level of the finite element model is fixed against displacement and rotation so that SSI is effectively disabled.
- **P-Delta Analysis** – This radio button allows the user to account for large displacement effects of axial loads in the above grade column elements using the corotational geometric transformation [3].

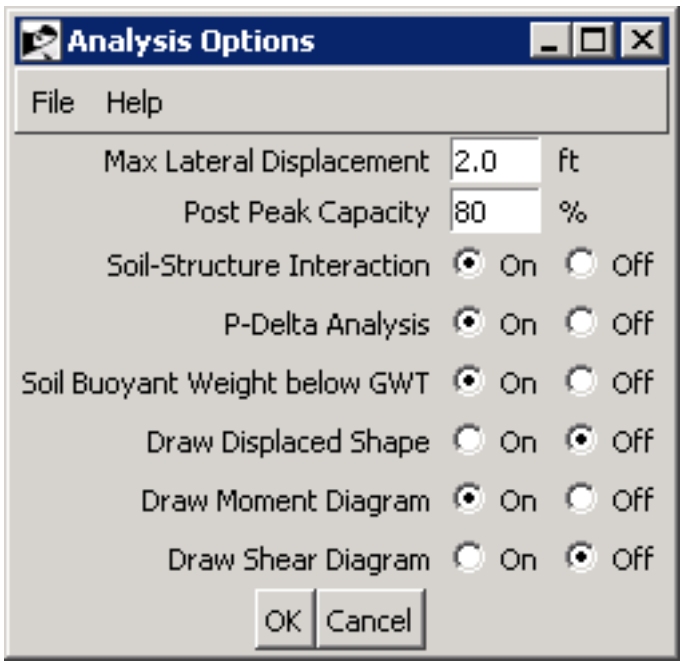

Figure 2.7: Analysis Options window showing software default values.

- **Soil Buoyant Weight below GWT** – This option tells the software whether or not to subtract the specific weight of water from the input soil properties for p-y springs that are below the water table.
- **Draw Displaced Shape** – To draw the displaced shape of the bent at each load step during the pushover analysis.
- **Draw Moment Diagram** – To draw the bending moment diagram (including locations of local extrema and points of inflection) at each load step during the pushover analysis.
- **Draw Shear Diagram** – To draw the sheare diagram (including locations of local extrema) at each load step during the pushover analysis.

Note that the three **Draw** options may be selected so that combinations, e.g., moment and shear diagram, are drawn simultaneously during the pushover analysis. By default, only the moment diagram is drawn.

2.5 Limit States

The software allows user-defined limit states to be tracked during the analysis for plotting in summary reports. As shown in Figure 2.8, three limit states are available to detect when peak strains are reached in the longitudinal reinforcing steel, jacket steel, and concrete.

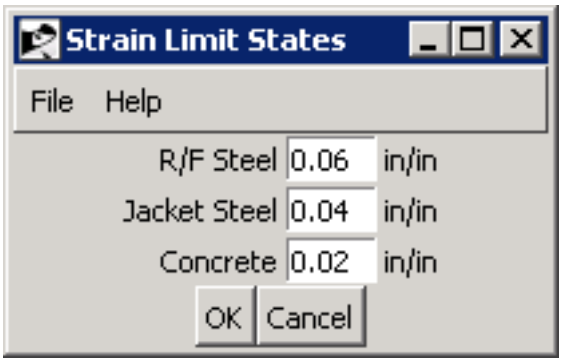

Figure 2.8: Limit States window showing software default values.

Chapter 3

Summary Report

The software will create a PDF report summarizing the bent's geometric and material properties in addition to analysis results. This feature is accessed by pressing the "Create Report" button shown on the main window in Figure 1.3 and gives the dialog box shown in Figure 3.1. The contents of the report, created from the software's default properties, are summarized in the following pages.

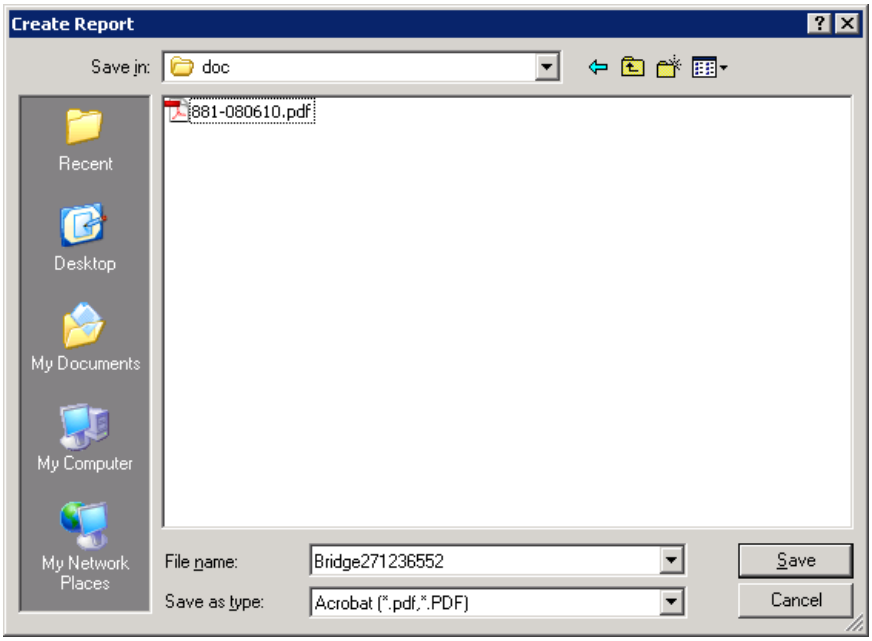

Figure 3.1: File dialog window to save PDF summary report.

3.1 Title Page and Table of Contents

The title page echoes information from the main window (Figure 1.3) including the bridge name, performing engineer, and date of analysis. There is also a table of contents as shown in Figure 3.2.

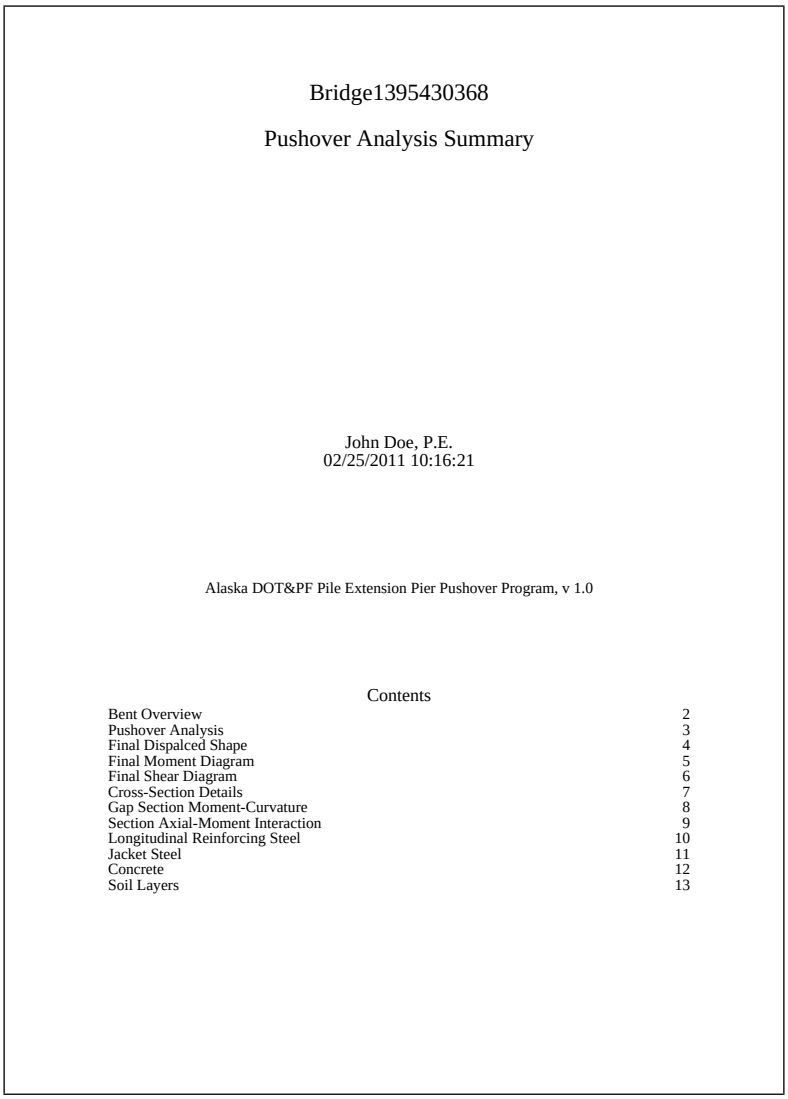

Bridge1395430368

Pushover Analysis Summary

John Doe, P.E.
02/25/2011 10:16:21

Alaska DOT&PF Pile Extension Pier Pushover Program, v 1.0

Contents

Figure 3.2: Sample title page of PDF summary report.

3.2 Bent Overview

A summary of bent dimensions is given on page 2 of the report. The summary includes column height, cap beam dimensions, shell gap, plastic hinge length, water table location, and total soil depth. A rendering (with limited color for better printing) of the bent model is included, as shown in Figure 3.3.

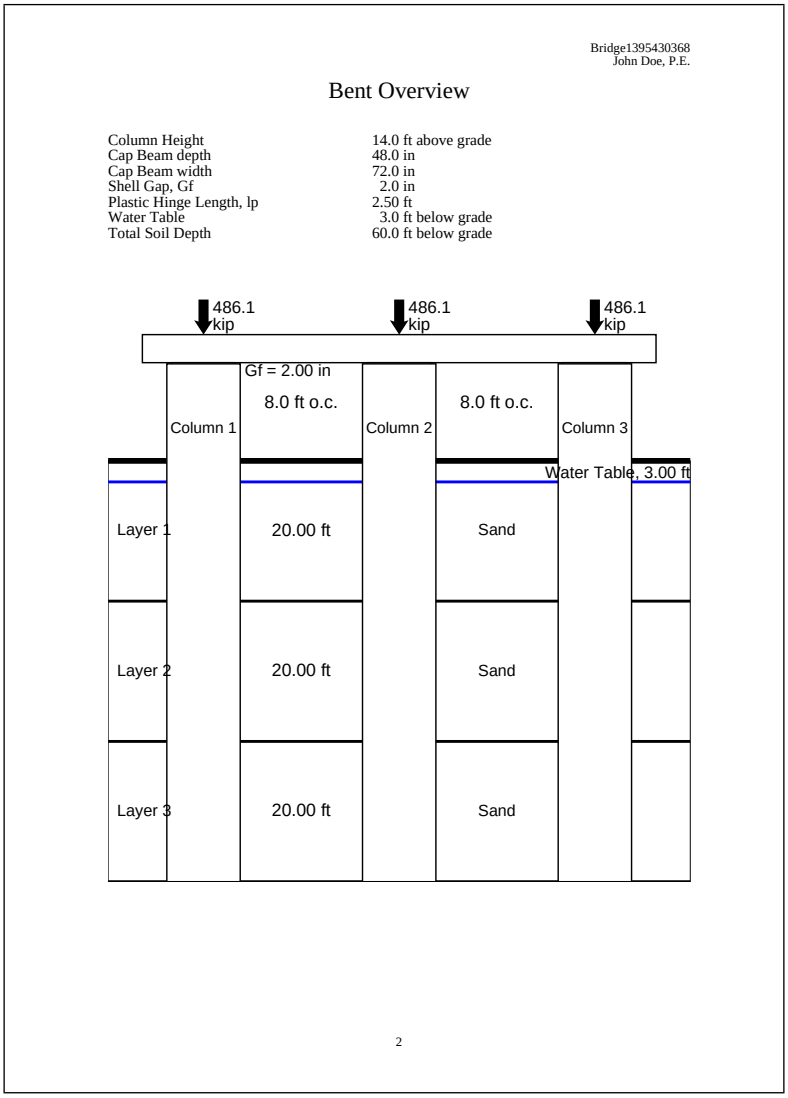

Figure 3.3: Sample bent overview of PDF summary report.

3.3 Pushover Analysis

The lateral load-displacement response of the bent is shown on page 3 of the report. In addition to the pushover curve, there is summary information regarding the selected analysis options and a summary of limit state information, as shown in Figure 3.4.

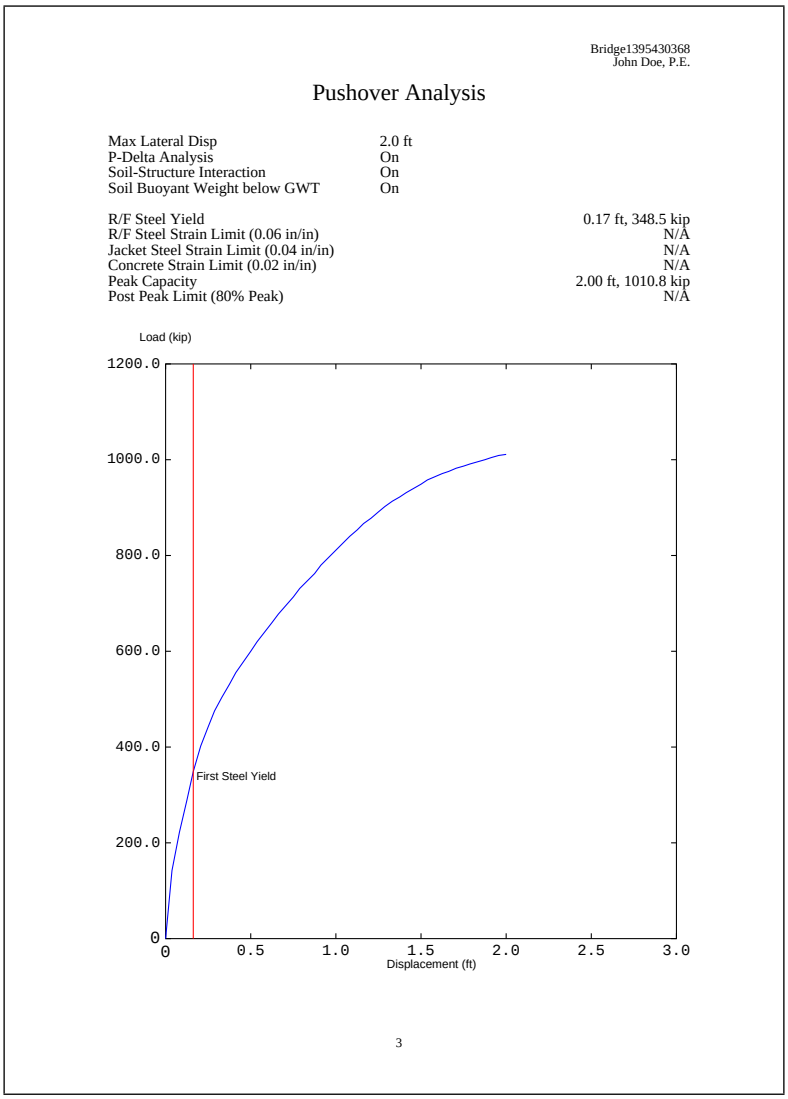

Figure 3.4: Sample pushover analysis of PDF summary report.

3.4 Final Displaced Shape

The displaced shape of the bent at the last load step of the pushover analysis is shown on page 4 of the report. In addition, the extreme minimum and maximum axial loads are summarized for each column, as shown in Figure 3.5.

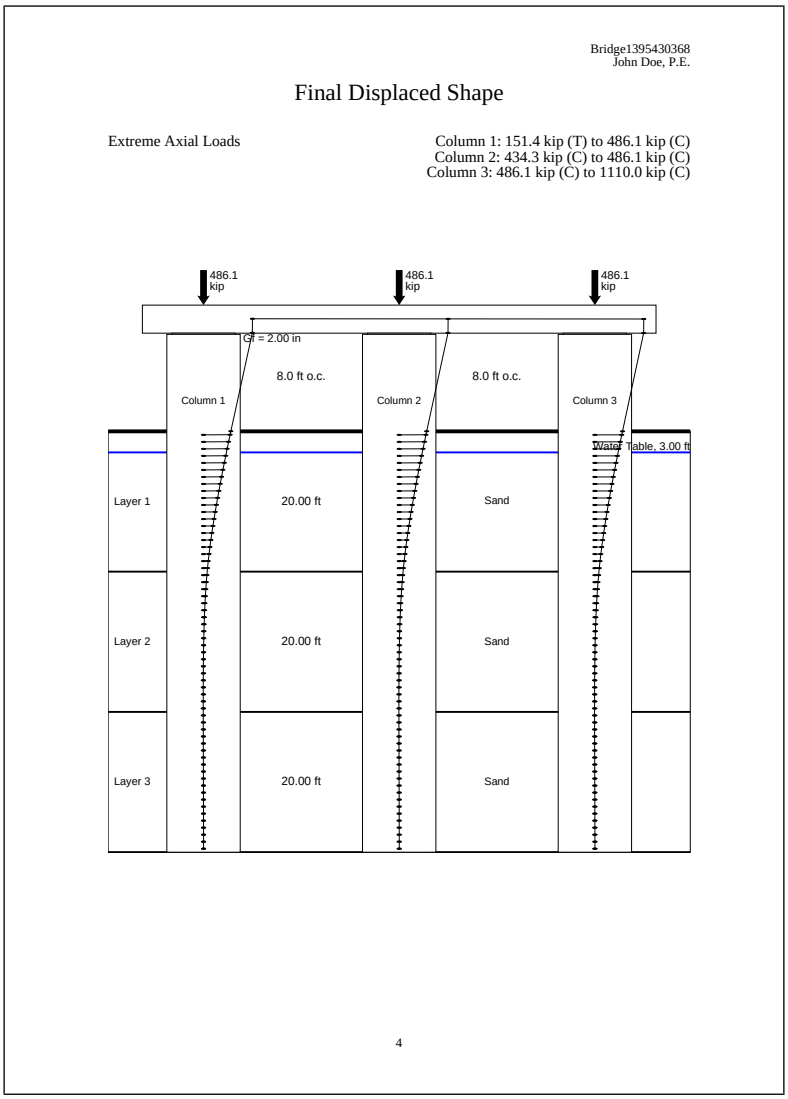

Figure 3.5: Sample displaced shape of PDF summary report.

3.5 Final Moment Diagram

The moment diagram for each pile at the last load step of the pushover analysis is shown on page 5. In addition, the magnitude and location of extreme bending moments and inflection point locations are labeled, as shown in Figure 3.6.

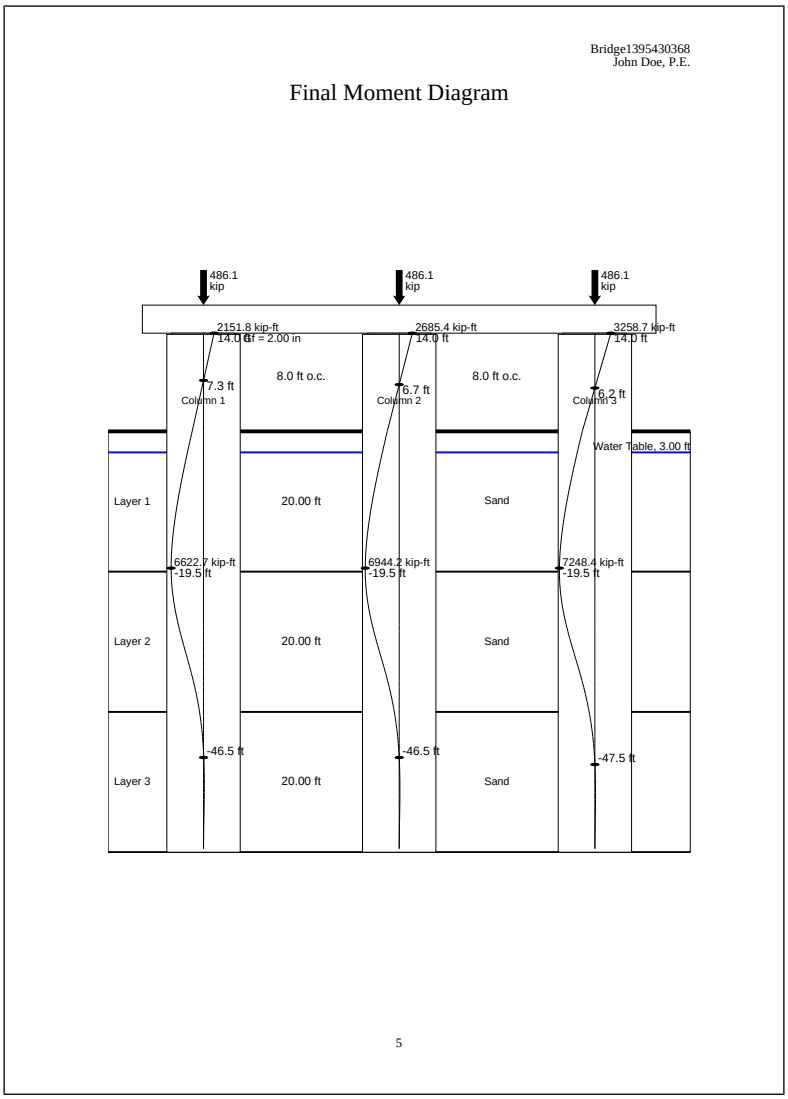

Figure 3.6: Sample moment diagram of PDF summary report.

3.6 Final Shear Diagram

The shear diagram for each pile at the last load step of the pushover analysis is shown on page 6. In addition, the magnitude and location of extreme shears and are labeled, as shown in Figure 3.7.

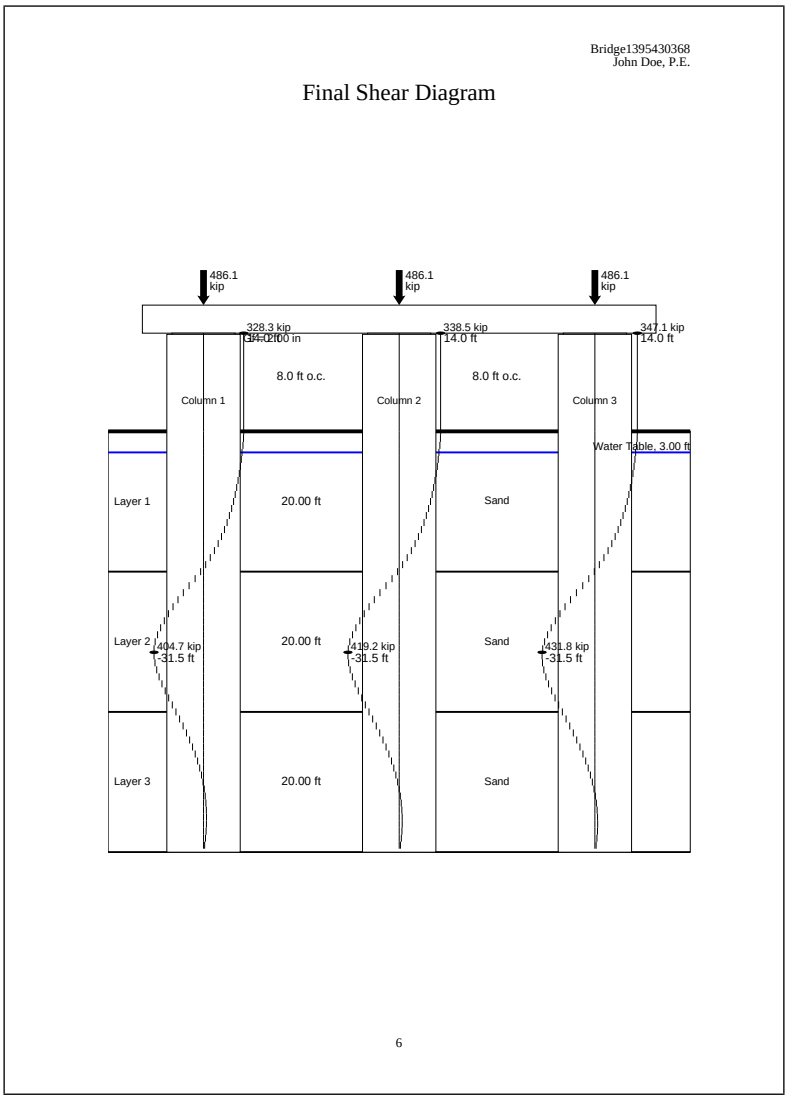

Figure 3.7: Sample shear diagram of PDF summary report.

3.7 Cross-Section Details

A summary of column/pile cross-section reinforcing details is shown on page 7. Presented information includes the outer diameter and thickness of the steel shell, the amount of cover concrete, and the number, size, and area ratio of longitudinal reinforcing bars. In addition, there is information on spiral reinforcement, which is not rendered in the report, as shown in Figure 3.8.

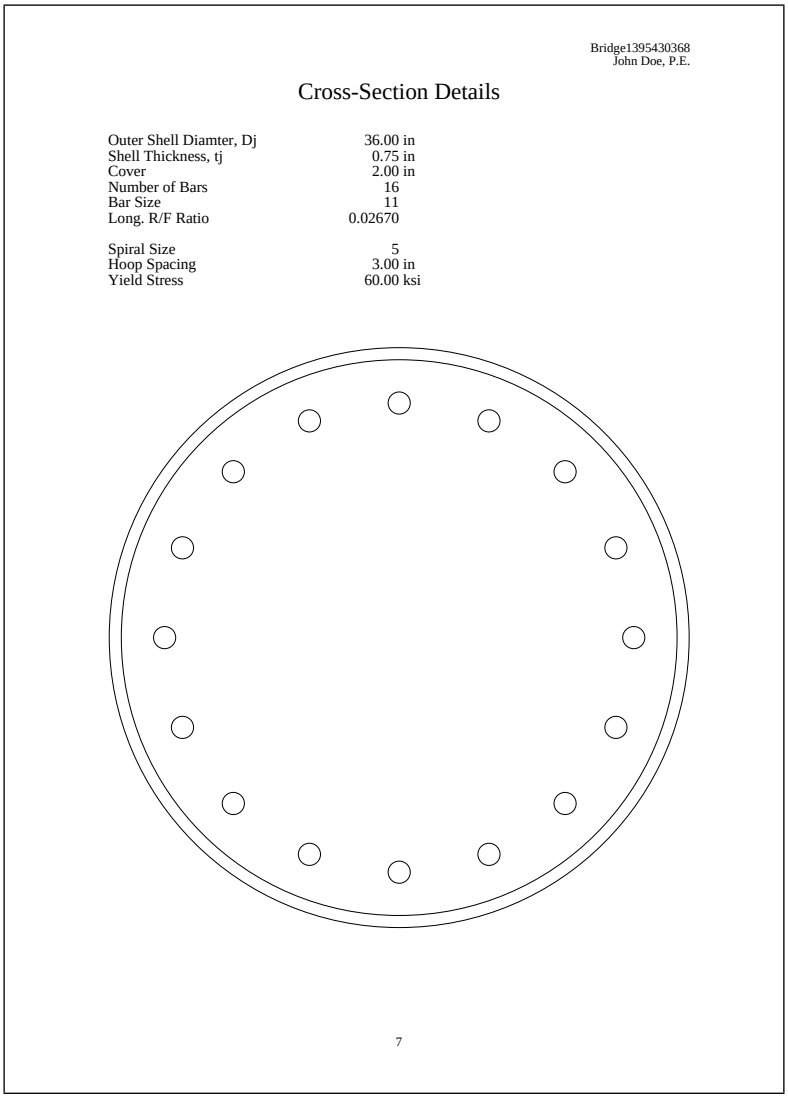

Figure 3.8: Sample cross-section details of PDF summary report.

3.8 Gap Section Moment-Curvature

Moment-curvature analysis of the gap section is presented on page 8, as shown in Figure 3.9. Analyses are shown for the overall extreme axial loads summarized on page 4 of the report (Figure 3.5). User-selected assumptions regarding the confinement of core and cover concrete in the gap region are also shown on this page of the report.

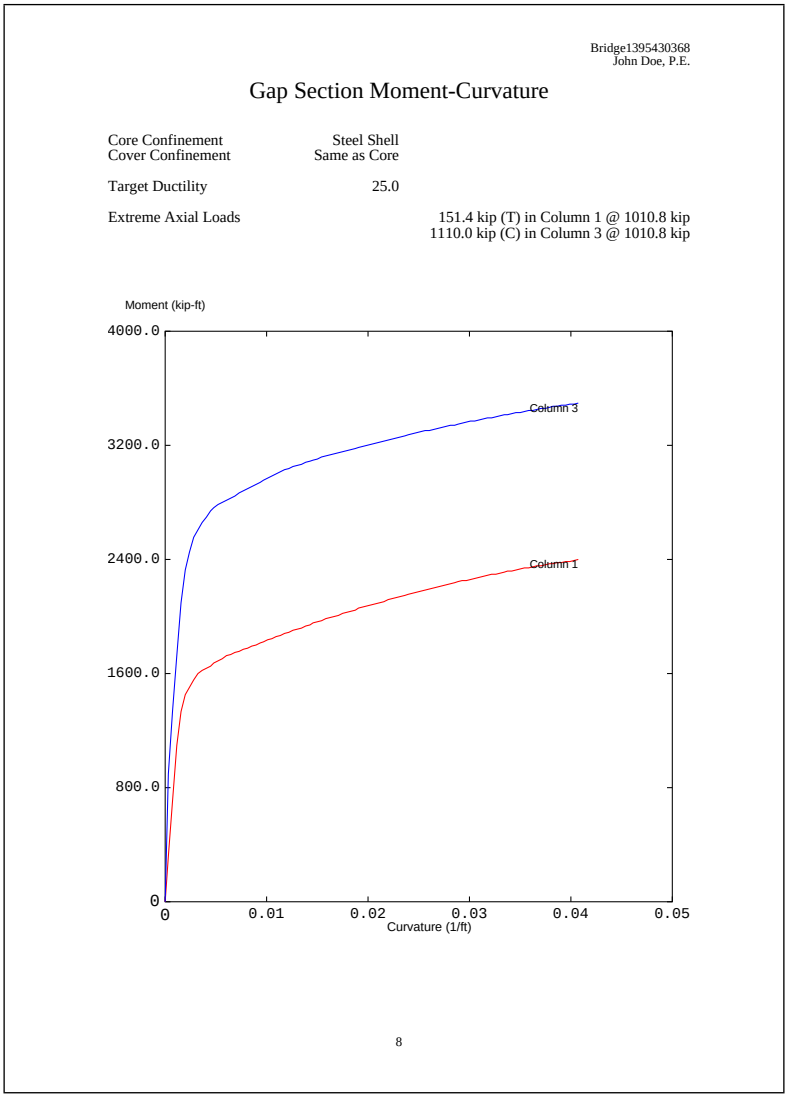

Figure 3.9: Sample moment-curvature analysis of PDF summary report.

3.9 Gap Section Axial-Moment Interaction

Axial-moment interaction of the gap and steel shell sections is presented on page 9, as shown in Figure 3.10. Balance point information is shown along with user-selected assumptions for the confinement of core and cover cocrete in the gap region.

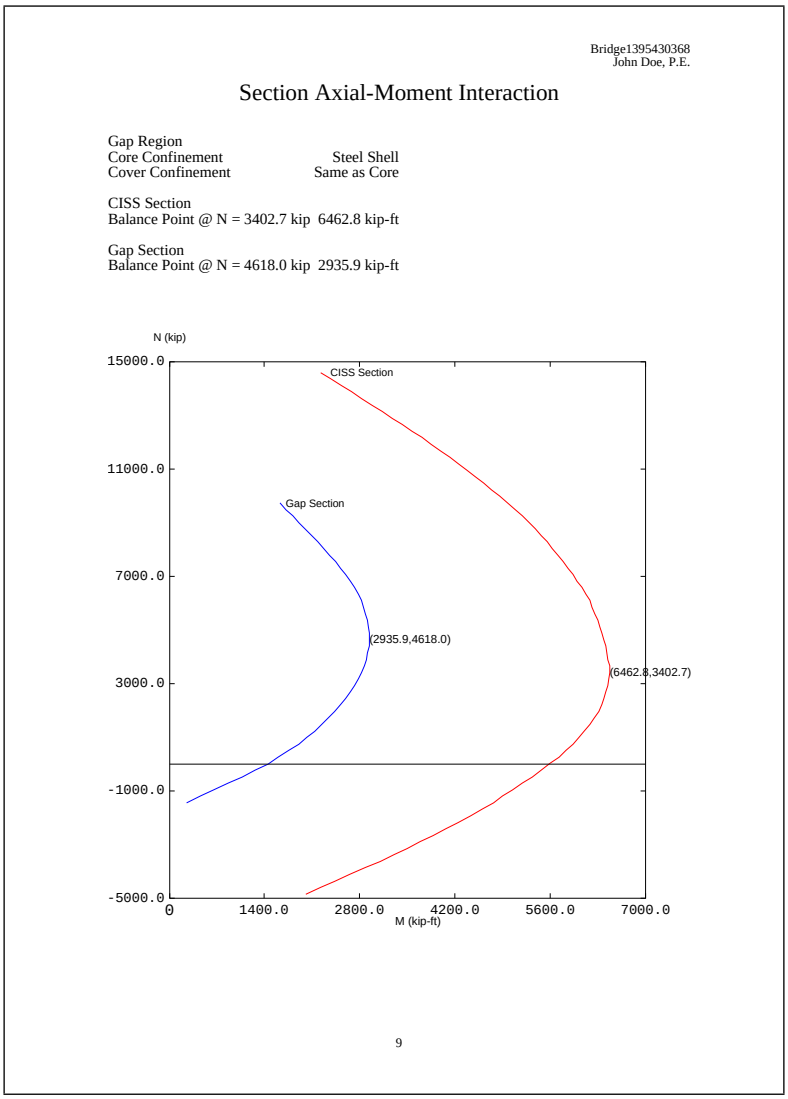

Figure 3.10: Sample axial-moment interaction of PDF summary report.

3.10 Steel Stress-Strain

Stress-strain curves for the longitudinal and jacket steel are shown on pages 10 and 11, respectively, along with a summary of physical properties, as shown in Figure 3.11.

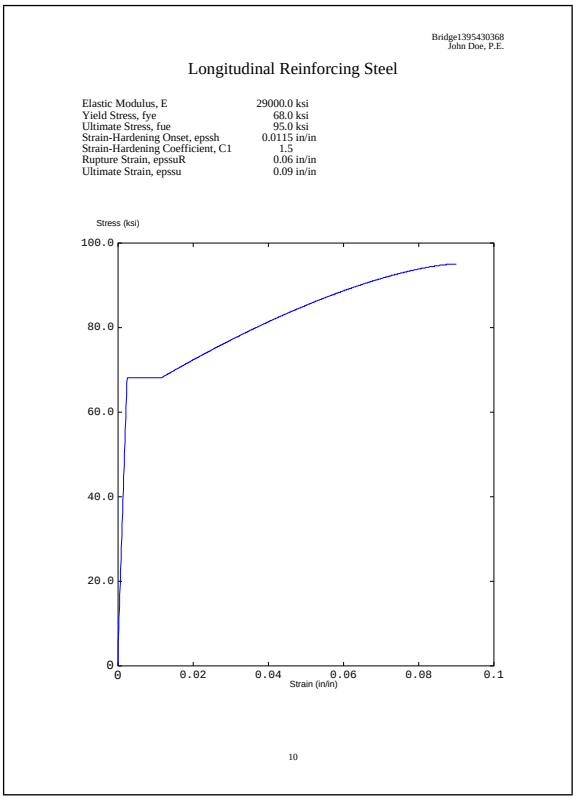

(a) Longitudinal steel

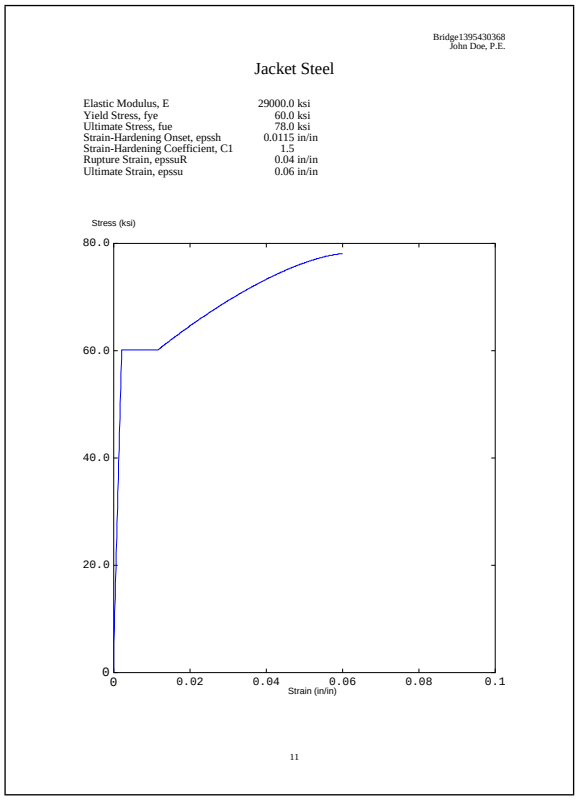

(b) Jacket steel

Figure 3.11: Sample steel stress-strain of PDF summary report.

3.11 Concrete Stress-Strain

Concrete stress-strain curves are presented on page 12. Three curves are shown, one each for unconfined, hoop-confined, and steel jacket confined concrete, as shown in Figure 3.12. In addition, physical properties used in obtaining each curve are shown at the top of the page.

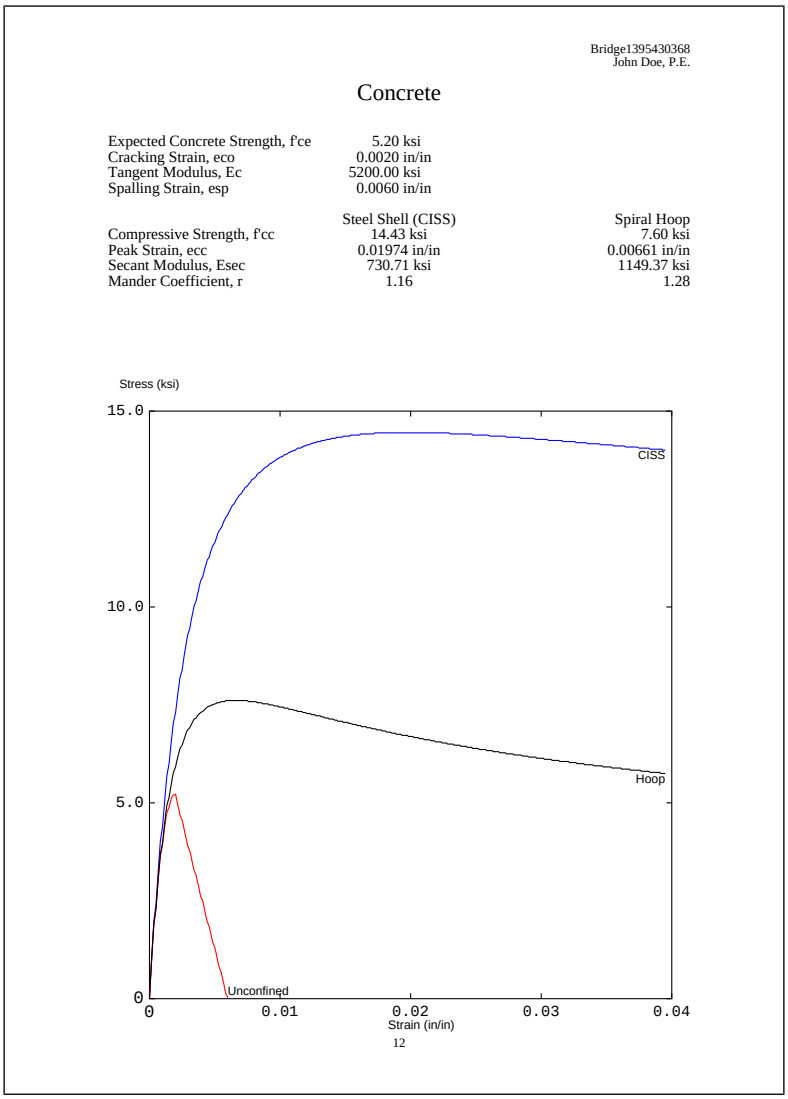

Figure 3.12: Sample concrete stress-strain of PDF summary report.

3.12 Soil p-y Curves

Resistance curves for each p-y spring are shown of the final pages of the report. The springs in layer 1 are shown on page 13, layer 2 on page 14, layer 3 on page 15, etc. The layer's soil type, depth, p-y spacing, number of springs, and physical properties are summarized at the top of the page, with a series of p-y curves plotted below, as shown in Figure 3.13.

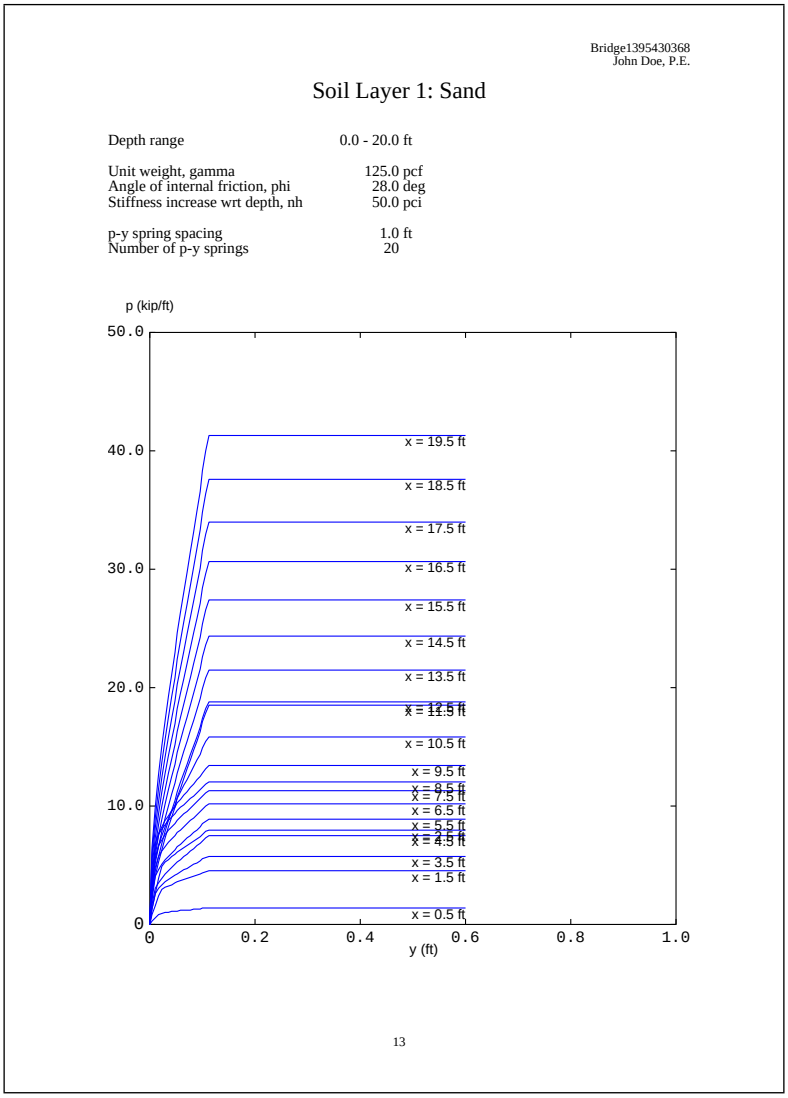

Figure 3.13: Sample soil p-y curves of PDF summary report.

Chapter 4

Future Extensions

Should use of this software become more prevalent by AKDOT&PF engineers, it is anticipated that additional features will have to be incorporated. Potential features include, but are not limited to the following:

- Different types of analysis procedures as seismic design provisions evolve.
- Incorporation of frozen soil p-y curves that are under development by other AKDOT&PF-sponsored researchers.
- Incorporation of specialized soil p-y curves based on user-defined input.
- Sensitivity and reliability options for quantifying epistemic and aleatory uncertainty of bent models and analysis assumptions.

Bibliography

[1] AASHTO. *Guide Specifications for LRFD Seismic Bridge Design*. American Association of State Highway and Transportation Officials, Washington, D.C., first edition, 2009.

[2] Y. H. Chai, M. J. N. Priestley, and F. Seible. Analytical model for steel-jacketed RC circular bridge columns. *Journal of Structural Engineering*, 120(8):2358–2376, 1994.

[3] M. A. Crisfield. *Non-linear Finite Element Analysis of Solids and Structures*, volume 1. John Wiley & Sons, 1991.

[4] D. C. Kent and R. Park. Flexural members with confined concrete. *Journal of the Structural Division, ASCE*, 97(7):1969–1990, 1971.

[5] J. B. Mander, M. J. N. Priestley, and R. Park. Theoretical stress-strain model for confined concrete. *Journal of Structural Engineering*, 114(8):1804–1826, August 1988.

[6] H. Matlock. Correlations for design of laterally loaded piles in soft clay. In *Second Annual Offshore Technology Conference*, volume 1, pages 577–594, Houston, TX, 1970.

[7] A. Neuenhofer and F. C. Filippou. Evaluation of nonlinear frame finite-element models. *Journal of Structural Engineering*, 123(7):958–966, July 1997.

[8] D. J. Raynor, D. L. Lehman, and J. F. Stanton. Bond slip response of reinforced bars grouted in ducts. *ACI Structural Journal*, 99(5), 2002.

[9] L. C. Reese, W. R. Cox, and F. D. Koop. Analysis of laterally loaded piles in sand. In *Fifth Annual Offshore Technology Conference*, number OTC 2080, Houston, TX, 1974. GESA Report No. D-75-9.

[10] L. C. Reese, W. R. Cox, and F. D. Koop. Field testing and analysis of laterally loaded piles in stiff clay. In *Seventh Offshore Technology Conference*, number OTC 2312, Houston, TX, 1975.

[11] M. H. Scott and G. L. Fenves. Plastic hinge integration methods for force-based beam-column elements. *Journal of Structural Engineering*, 132(2):244–252, February 2006.

[12] S.-T. Wang and L. C. Reese. COM624P – Laterally loaded pile analysis program for the microcomputer. Technical Report FHWA-SA-91-048, Federal Highway Administration, Washington, DC, 1993.